A 3-RRRS PARALLEL STRUCTURE FOR MEASURING ROBOT PATH

Glicerinho Danter Lopes Soares Júnior, gliglijr@hotmail.com
João Carlos Mendes Carvalho, e-mail, jcmendes@mecanica.ufu.br
Rogério Sales Gonçalves, rsgoncalves@mecanica.ufu.br
UFU, Universidade Federal de Uberlândia, Curso de Engenharia Mecatrônica, Campus Santa Mônica, Bairro Santa Mônica, CEP 38400-902, Uberlândia, Minas Gerais

Abstract. *Multibody systems consist on a kinematic chain composed of links that can be rigid or flexible, interconnected by joints. The multibody systems are of great importance and are used in various applications such as in aerospace and automotive, machine tools, mechanisms, sea exploration, medicine and robotics. A robotic structure can be defined as a multibody system. Despite the research carried, there is still no system capable of verifying the trajectory described by its end-effector, during its evolution in the workspace. This paper attempts to develop an electro-mechanical system using as the base the parallel structure 3-RRRS, where the passive revolute joints are coupled to potentiometers, whose signals are acquired by a data acquisition board, connected to a computer. These signals are properly processed and converted, through the geometric model of parallel structure 3-RRRS, in the position and orientation of the mobile platform. This mobile platform can be connected to the end-effector robot to verify the robot path, comparing the position and orientation commanded to the robot with those obtained by the measurement structure 3-RRRS. Thus, in this paper are presented the direct geometric models, the Jacobian matrix, analysis of geometric errors, the influence of each revolute joint errors on the quality of measurement and data acquisition. Finally experimental tests are conducted in a commercial measurement three-dimensional structure.*

Keywords*: Multibody Systems, Robotic Structures, 3-RRRS Parallel Structure, Measure.*

1. INTRODUCTION

Robotic structures may be defined as multibody systems, composed of segments, rigid or flexible, interconnected by joints. Multibody systems can be classified as serial kinematic chain, in which segments are connected in series one by one from the base to the end-effector, parallel kinematic chain, in which exist two or more serial kinematic chains connecting the base to the end-effector, and hybrid kinematic chain, which is the combination of the above (Tsai, 1999; Gonçalves, 2009).

Robotic structures have many applications in various fields such as aviation, maritime exploration, medical and automotive. Few literature studies describe equipment for verification of robot trajectories. Oliveira and Carvalho (2002) perform the measurement of robot path with a modified parallel structure based on Stewart platform to realize the indirect measurement of position and orientation. Several other studies apply the measure of displacement, but in systems with micro-positioning. Fan and Chen (1999) developed a system to measure micro-displacement employing four laser Doppler scales and two quadrant photo detectors to detect the positions and the rotations of an optical reflection device. Wu and Chuang (2004) developed a compact roll angular displacement measurement system based on measuring the phase difference between the reference and measurement lasers beams. Kim *et al*. (2002) use a six degree-of-freedom (d.o.f.) displacement measurement system using detection of the movement of rays reflected from various cooperative targets that relies upon optical triangulation and optical beam deflection method. Other works show applications to measure only rotation, like Zangl *et al*. (2007), that propose the study on the use of an array of lateral hall elements for the implementation of a three-axial Joystick, that can measure rotation about one axis and measure or detect positions of the tilt along the remaining horizontal axes.

In this way, this paper proposes the development of an electromechanical system using the parallel structure 3-RRRS able to perform measurements of paths providing the position and orientation of the moving platform or end-effector.

2. 3-RRRS PARALLEL STRUCTURE

The parallel structure 3-RRRS has a triangular base and a triangular moving platform. Connecting the base vertices and the moving platform vertices are RRRS serial chains (from a passive revolute joint at the base, the segments are connected serially by two other passive revolute joints and connected to the end-effector by a spherical joint), Fig. 1(a). In this first model, all structure was assembled using parts from the kit Lego Mindstorm NXT. The use of these parts is justified by its tolerance manufacturing, ensuring dimensional homogeneity of the elements, and easy of assembly, besides the low weight of the parts. The Lego pieces flexibility was neglected. The sketch of the 3-RRRS structure is shown in Fig. 1 (a) and layout of the structure built with pieces of kit Lego is shown in Fig. 1 (b). $\boldsymbol{X}$, $\boldsymbol{Y}$ and $\boldsymbol{Z}$ are the axes of the inertial frame at the origin O fixed at the base center and $\boldsymbol{x}$, $\boldsymbol{y}$ and $\boldsymbol{z}$ are the axes of frame at the origin A fixed at the moving platform center, A_i are the vertices of the moving platform in which the leg i is connected, d_j represents the length of the segment posterior joint j and the notation ij represents the j-th joint of i-th leg.

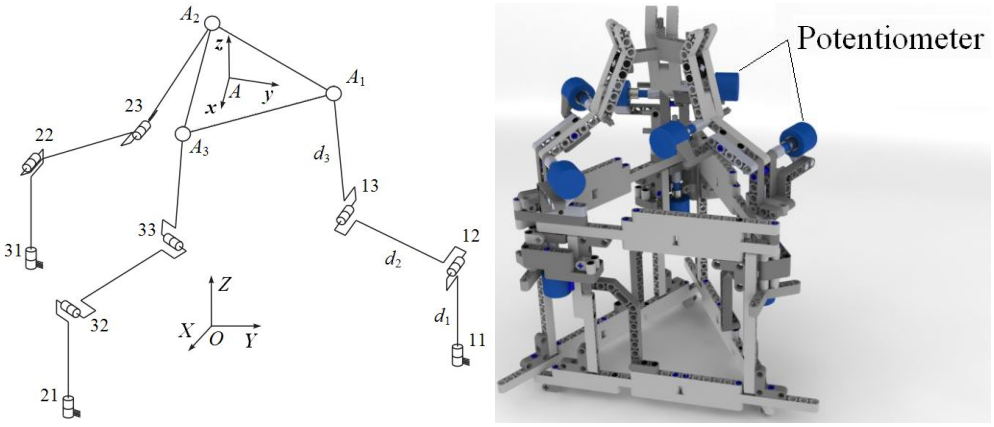

(a) (b)

Figure 1. a) Sketch of 3-RRRS structure; b) 3-RRRS structure assembled with pieces of kit Lego.

By moving the mobile platform of the structure 3-RRRS variations occur in the angles of joints, using potentiometers attached to each passive revolute joint, Fig. 1 (b), can be measured these angles and, from the direct geometric model, to obtain the position and orientation of the moving platform.

2.1. Angles measurement system

The read of the each passive revolute joint angles of 3-RRRS was realized indirectly through read the voltage in the potentiometers coupled in the passive revolute joints, were used precision potentiometers Baotou 3590S-103, 10kΩ - 10 turns in series with a 390Ω resistor, connected with a source model HP 6653A 50V/30A. The read voltage was performed by a data acquisition card NI USB-6211 16 bit - 250kS/s and LabView software to interface with the data acquisition card and the signal processing. The configuration series of the potentiometer with the resistor increases significantly the system sensitivity in the desired range. Figure 2 shows the voltage on the potentiometer by its resistance, using the 390Ω resistor and can be noted that in the half of the first lap of the potentiometer the voltage reaches 56% of the voltage provided by the source, making more precise measurements and minimizing the effects of external noise on the signal.

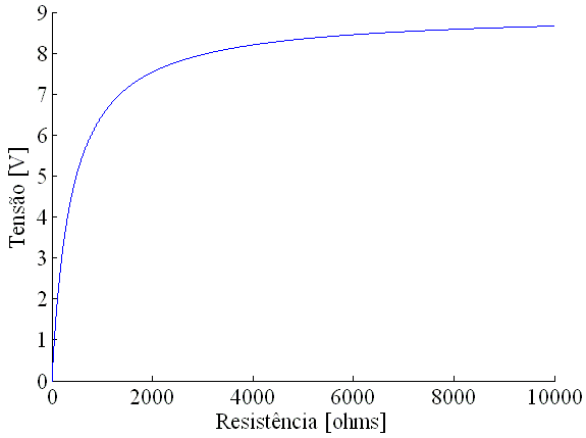

Figure 2. Voltage on the potentiometer by its resistance

The calibration of the potentiometers was done during the assembly of the structure, after each potentiometer being coupled to its respective passive revolute joint. With a protractor with 1 degree resolution, was done the calibration of the potentiometer, with an increase of one degree along your angle work, using the data acquisition card NI USB-6211.

After the acquisition, through the LabView software, the signal passes through a low pass filter 2nd order Butterworth, implemented digitally, and is converted from voltage to degrees using the equation of the series circuit. The program allows save the desired number of measurement and using Matlab software from the direct geometric model implemented is possible obtain the moving platform position and orientation.

2.2. Forward geometric model of 3-RRRS structure

From the structure configuration, i.e. the angles of each passive revolute joint, is possible determine the moving platform position and orientation using Homogeneous Transformation Matrices (HTM).

The sequence of linear transformations performed from the inertial frame in a serial chain structure (leg) to a vertex of the moving platform is shown in Fig. 3. Where $\boldsymbol{x_{ij}}$, $\boldsymbol{y_{ij}}$ and $\boldsymbol{z_{ij}}$ represent generalizations of the linear transformations that occurred in the change of inertial frame to the joint j of leg i, the notation " ´ " means a change in the orientation of reference; q_{ij} represents the angle of joint j of leg i and x_i, y_i and z_i indicate the orientation of the vertex A_i.

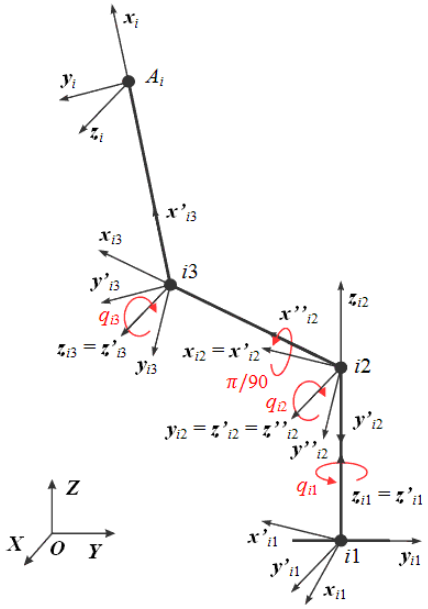

Figure 3. Linear transformations from the inertial frame to the moving platform.

Equation (1) presents the transformations to perform the change of inertial frame to the point *Ai*, as shown in Fig. 3.

$$\boldsymbol{pa}_i = \boldsymbol{p}_{i1}\begin{bmatrix} c\,q_{i1} & -s\,q_{i1} & 0 & 0 \\ s\,q_{i1} & c\,q_{i1} & 0 & 0 \\ 0 & 0 & 1 & 0 \\ 0 & 0 & 0 & 1 \end{bmatrix}\begin{bmatrix} 1 & 0 & 0 & 0 \\ 0 & 1 & 0 & 0 \\ 0 & 0 & 1 & d_1 \\ 0 & 0 & 0 & 1 \end{bmatrix}\begin{bmatrix} 1 & 0 & 0 & 0 \\ 0 & 0 & 1 & 0 \\ 0 & -1 & 0 & 0 \\ 0 & 0 & 0 & 1 \end{bmatrix}\begin{bmatrix} c\,q_{i2} & -s\,q_{i2} & 0 & 0 \\ s\,q_{i2} & c\,q_{i2} & 0 & 0 \\ 0 & 0 & 1 & 0 \\ 0 & 0 & 0 & 1 \end{bmatrix}\begin{bmatrix} 1 & 0 & 0 & d_2 \\ 0 & 1 & 0 & 0 \\ 0 & 0 & 1 & 0 \\ 0 & 0 & 0 & 1 \end{bmatrix}\begin{bmatrix} c\,q_{i3} & -s\,q_{i3} & 0 & 0 \\ s\,q_{i3} & c\,q_{i3} & 0 & 0 \\ 0 & 0 & 1 & 0 \\ 0 & 0 & 0 & 1 \end{bmatrix}\begin{bmatrix} 1 & 0 & 0 & d_3 \\ 0 & 1 & 0 & 0 \\ 0 & 0 & 1 & 0 \\ 0 & 0 & 0 & 1 \end{bmatrix} \quad (1)$$

Where $\boldsymbol{pa}_i$ is a HTM that contains the position and orientation of the vertex i of the moving platform, $\boldsymbol{p}_{i1}$ represents the HTM of inertial frame to the reference in the joint $i1$, c and s represent the cosine and sine, respectively, of the angles q_{ij} and rb is the radius of base. Equation (2) shows the HTM to the vertices of the base, the joints 1 of the legs 1, 2 and 3.

$$\boldsymbol{p}_{11} = \begin{bmatrix} 1 & 0 & 0 & 0 \\ 0 & 1 & 0 & rb \\ 0 & 0 & 1 & 0 \\ 0 & 0 & 0 & 1 \end{bmatrix}, \boldsymbol{p}_{21} = \begin{bmatrix} 1 & 0 & 0 & -rb\,s\,120^o \\ 0 & 1 & 0 & rb\,c\,120^o \\ 0 & 0 & 1 & 0 \\ 0 & 0 & 0 & 1 \end{bmatrix} \text{ e } \boldsymbol{p}_{31} = \begin{bmatrix} 1 & 0 & 0 & -rb\,s\,-120^o \\ 0 & 1 & 0 & rb\,c\,-120^o \\ 0 & 0 & 1 & 0 \\ 0 & 0 & 0 & 1 \end{bmatrix} \quad (2)$$

From the position of the vertices of the end-effector, given by HTM $\boldsymbol{pa}_1$, $\boldsymbol{pa}_2$ and $\boldsymbol{pa}_3$, and the condition that the reference moving platform is located at the center of triangular platform is possible obtain the position of the moving platform $\boldsymbol{pa}$, Eq (3).

$$\boldsymbol{pa} = \begin{bmatrix} 1 & 0 & 0 & 0 \\ 0 & 1 & 0 & 0 \\ 0 & 0 & 1 & 0 \end{bmatrix} * \frac{\boldsymbol{pa}_1 + \boldsymbol{pa}_2 + \boldsymbol{pa}_3}{3} * \begin{bmatrix} 0 \\ 0 \\ 0 \\ 1 \end{bmatrix} \quad (3)$$

Equation (4) provides the $\boldsymbol{y}$ axis, located in the reference fixed at the moving platform center, from the condition of that it points to the vertex A_1.

$$\boldsymbol{y} = \frac{\boldsymbol{pa_1} - \boldsymbol{pa}}{\|\boldsymbol{pa_1} - \boldsymbol{pa}\|} \tag{4}$$

Equation (5) gives the $\boldsymbol{x}$ axis from the condition of that it is parallel to segment $\overline{\boldsymbol{pa_2}\,\boldsymbol{pa_3}}$.

$$\boldsymbol{x} = \frac{\boldsymbol{pa_3} - \boldsymbol{pa_2}}{\|\boldsymbol{pa_3} - \boldsymbol{pa_2}\|} \tag{5}$$

Equation (6) gives the $\boldsymbol{z}$ axis perpendicular to the axes $\boldsymbol{x}$ and $\boldsymbol{y}$.

$$\boldsymbol{z} = \boldsymbol{x} \times \boldsymbol{y} \tag{6}$$

The orientation matrix of the moving platform, $\boldsymbol{Ra}$, is composed by the orientation of the axes of reference attached to the moving platform, Eq (7).

$$\boldsymbol{Ra} = [\boldsymbol{x}\ \boldsymbol{y}\ \boldsymbol{z}]_{3x3} \tag{7}$$

The matrix containing the position and orientation of the end-effector, $\boldsymbol{pA}$, is the combination of the matrix of orientation $\boldsymbol{Ra}$ and of the position vector $\boldsymbol{pa}$, Eq (8).

$$\boldsymbol{pA} = \begin{bmatrix} \boldsymbol{Ra} & \boldsymbol{pa} \\ 0 & 1 \end{bmatrix}_{4x4} \tag{8}$$

Similarly to the direct geometric model, the inverse geometric model was obtained using HTM.

2.3. Jacobian matrix

The Jacobian matrix *J* is a linear transformation matrix that allows to relate the infinitesimal changes of generalized coordinates with the infinitesimal changes of coordinates operational, i.e., the element (*k*, *l*) of Jacobian matrix describes as a differential change in the coordinate q_l affects differential change of operational coordinates x_k, so, the Jacobian is dependent on the configuration of the robot and is given by Eq. (9).

$$\delta\boldsymbol{x} = \boldsymbol{J}\,\delta\boldsymbol{q} \tag{9}$$

Where $\delta\boldsymbol{x}$ is the column vector containing the differentials of the operational coordinates, Eq. (10).

$$\delta\boldsymbol{x} = [\,\delta x_a\ \delta y_a\ \delta z_a\ \delta x_x\ \delta x_y\ \delta x_z\ \delta y_x\ \delta y_y\ \delta y_z\ \delta z_x\ \delta z_y\ \delta z_z]^{\mathrm{T}} \tag{10}$$

Where δx_a, δy_a e δz_a are the differentials of the operational coordinates, components of the position $\boldsymbol{pA}$ and δx_x, δx_y, δx_z, δy_x, δy_y, δy_z, δz_x, δz_y and δz_z are the differentials of the components of the matrix of orientation $\boldsymbol{Ra}$.

And $\delta\boldsymbol{q}$ is the column vector containing the differentials of the generalized coordinates, Eq (11).

$$\delta\boldsymbol{q} = [\,\delta q_{11}\ \delta q_{12}\ \delta q_{13}\ \delta q_{21}\ \delta q_{22}\ \delta q_{23}\ \delta q_{31}\ \delta q_{32}\ \delta q_{33}]^{\mathrm{T}} \tag{11}$$

The Jacobian matrix is obtain by

$$\boldsymbol{J} = \begin{bmatrix} \frac{\delta x_a}{\delta q_{11}} & \cdots & \frac{\delta x_a}{\delta q_{33}} \\ \frac{\delta y_a}{\delta q_{11}} & \cdots & \frac{\delta y_a}{\delta q_{33}} \\ \vdots & \ddots & \vdots \\ \frac{\delta z_y}{\delta q_{11}} & \cdots & \frac{\delta z_y}{\delta q_{33}} \\ \frac{\delta z_z}{\delta q_{11}} & \cdots & \frac{\delta z_z}{\delta q_{33}} \end{bmatrix}_{12x9} \tag{12}$$

From Eqs. (9) to (12) can be obtained Eq. (13).

$$\begin{aligned} \delta x_{a_l} &= J_{1l} * \delta q_l \\ \delta y_{a_l} &= J_{2l} * \delta q_l \\ &\vdots \qquad (i = 1, \ldots, 9) \\ \delta z_{yl} &= J_{11l} * \delta q_l \\ \delta z_{zl} &= J_{12l} * \delta q_l \end{aligned} \tag{13}$$

That can calculate the contribution of error due to *l*-th joint. Thus, the position geometric error in the read of the vector ***pA*** due to *l*-th joint, e_{pl}, is given by Eq. (14).

$$e_{pl} = \sqrt{(\delta x_{al})^2 + (\delta y_{al})^2 + (\delta z_{al})^2} = \delta q_l * \sqrt{J_{1l}{}^2 + J_{2l}{}^2 + J_{3l}{}^2} = \delta q_l * \mu_{pl} \quad (14)$$

Where the parameter μ_{pl} represents the index of position sensitivity due to the *l*-th joint.

The absolute error in measuring the position, according to Alves (1996), is given by Eq. (15).

$$e_p = \sqrt{(\delta x)^2 + (\delta y)^2 + (\delta z)^2} = \sqrt{(x'_a - x_a)^2 + (y'_a - y_a)^2 + (z'_a - z_a)^2} \quad (15)$$

Where x_a, y_a and z_a are the default values and x'_a, y'_a and z'_a are values of position achieved by the structure in a known configuration.

Similar to the position geometric error, the contribution of orientation geometric error due to *l*-th joint, e_{ol}, is given by Eq. (16).

$$e_{ol} = \sqrt{(\delta x_{xl})^2 + \left(\delta x_{yl}\right)^2 + \cdots + \left(\delta z_{yl}\right)^2 + (\delta z_{zl})^2} = \delta q_l * \sqrt{J_{4l}{}^2 + \cdots + J_{12l}{}^2} = \delta q_l * \mu_{ol} \quad (16)$$

And the absolute error on measurement of the orientation is given by Eq. (17).

$$e_0 = \sqrt{(x_x{}' - x_x)^2 + \left(x_y{}' - x_y\right)^2 + \cdots + \left(z_y{}' - z_y\right)^2 + (z_z{}' - z_z)^2} \quad (17)$$

The Jacobian matrix of the 3-RRRS structure was solved using the Matlab software.

2.3. Analysis of geometric errors

Known equations of the forward geometric model the estimation of the errors present in the position and orientation of the vector ***pA***, assuming that the structure is rigid were carried out.

To determine the errors introduced by the mechanical structure and the signal acquisition system was used a computer model, where two values are obtained, one corresponding to a path inside the workspace of the structure in a configuration set to true and another value with an estimated error inserted computationally.

The error analysis was performed using an error value estimated from the components of the measurement system. The potentiometers used, due the calibration, have resolution of 1º; to the acquisition system, oscillations of 1mV in the signal acquired of the potentiometers, due to external noise, cause variations of up to 0.25 °, depending on the angle at which be in the potentiometer. To perform the analysis of geometric errors was used an error of 1º in each passive revolute joint.

Table 1 shows the data concerning to the operational coordinates and in the Tab. 2 shows the data concerning the generalized coordinates, of points along the working space, both being regarded as true.

Table 1. Measures of operational coordinates throughout the workspace considered true.

Pos.	x_x	x_y	x_z	y_x	y_y	y_z	z_x	z_y	z_z	x [mm]	y [mm]	z [mm]
1	1,0	0,0	0,0	0,0	0,997	0,082	0,000	-0,082	0,997	10,607	0,000	70,393
2	1,0	0,0	0,0	0,0	0,996	0,089	0,000	-0,089	0,996	15,000	0,000	81,000
3	1,0	0,0	0,0	0,0	0,995	0,095	0,000	-0,095	0,995	10,607	0,000	91,607
4	1,0	0,0	0,0	0,0	0,995	0,102	0,000	-0,102	0,995	0,000	10,607	70,393
5	1,0	0,0	0,0	0,0	0,994	0,109	0,000	-0,109	0,994	0,000	15,000	81,000
6	1,0	0,0	0,0	0,0	0,993	0,116	0,000	-0,116	0,993	0,000	10,607	91,607
7	1,0	0,0	0,0	0,0	0,992	0,123	0,000	-0,123	0,992	-10,607	0,000	70,393
8	1,0	0,0	0,0	0,0	0,992	0,129	0,000	-0,129	0,992	-15,000	0,000	81,000
9	1,0	0,0	0,0	0,0	0,991	0,136	0,000	-0,136	0,991	-10,607	0,000	91,607
10	1,0	0,0	0,0	0,0	0,990	0,143	0,000	-0,143	0,990	0,000	-10,607	70,393
11	1,0	0,0	0,0	0,0	0,989	0,150	0,000	-0,150	0,989	0,000	-15,000	81,000
12	1,0	0,0	0,0	0,0	0,988	0,156	0,000	-0,156	0,988	0,000	-10,607	91,607

Table 2. Measures of generalized coordinates throughout the workspace considered true.

Pos.	q_{11} [°]	q_{12} [°]	q_{13} [°]	q_{21} [°]	q_{22} [°]	q_{23} [°]	q_{31} [°]	q_{32} [°]	q_{33} [°]
1	279,78	-7,32	-59,88	25,73	-9,98	-41,24	144,17	-0,65	-83,19
2	283,70	-23,29	-36,08	24,28	-32,43	0,00	141,15	-12,96	-74,41
3	279,78	-44,58	0,00	25,75	-39,33	0,00	144,15	-27,78	-47,14
4	270,00	-4,61	-81,48	37,88	-6,45	-52,14	142,12	-6,45	-52,14
5	270,00	-17,47	-72,20	40,72	-27,88	-14,17	139,28	-27,88	-14,17
6	270,00	-33,61	-39,74	37,89	-40,61	0,00	142,11	-40,61	0,00
7	260,23	-8,62	-58,14	35,88	-0,07	-83,73	154,23	-9,32	-42,05
8	256,32	-25,16	-32,82	38,90	-12,36	-75,14	155,68	-32,15	0,00
9	260,24	-44,98	0,00	35,90	-27,03	-48,30	154,21	-39,08	0,00
10	270,00	-19,26	-24,67	20,82	-0,65	-76,24	159,18	-0,65	-76,24
11	270,00	-34,26	0,00	16,59	-13,14	-63,97	163,41	-13,14	-63,97
12	270,00	-41,06	0,00	20,85	-29,07	-37,73	159,15	-29,07	-37,73

Similar to the Tabs. 1 and 2, Tabs. 3 and 4 present the data concerning the operational and generalized coordinates, respectively, of points throughout the workspace, with the errors inserted.

Table 3. Measures of operational coordinates throughout the workspace with inserted error.

Pos.	x_x	x_y	x_z	y_x	y_y	y_z	z_x	z_y	z_z	x [mm]	y [mm]	z [mm]
1	1,0	0,0	0,0	0,0	0,991	0,131	-0,001	-0,131	0,990	10,294	0,616	70,174
2	1,0	0,0	0,0	0,0	0,990	0,135	-0,001	-0,135	0,990	14,727	0,746	80,791
3	1,0	0,0	0,0	0,0	0,990	0,134	0,000	-0,134	0,990	10,295	0,917	91,381
4	1,0	0,0	0,0	0,0	0,988	0,152	0,000	-0,152	0,988	-0,296	11,299	70,175
5	1,0	0,0	0,0	0,0	0,988	0,156	0,000	-0,156	0,988	-0,269	15,899	80,820
6	1,0	0,0	0,0	0,0	0,987	0,157	0,000	-0,157	0,987	-0,294	11,635	91,448
7	1,0	0,0	0,0	0,0	0,985	0,171	0,002	-0,171	0,985	-11,008	0,742	70,172
8	1,0	0,0	0,0	0,0	0,985	0,173	0,001	-0,173	0,985	-15,439	0,925	80,786
9	1,0	0,0	0,0	0,0	0,984	0,174	0,001	-0,174	0,985	-11,006	1,039	91,379
10	1,0	0,0	0,0	0,0	0,981	0,190	0,000	-0,190	0,981	-0,419	-9,903	70,154
11	1,0	0,0	0,0	0,0	0,980	0,193	0,000	-0,193	0,980	-0,444	-14,187	80,755
12	1,0	0,0	0,0	0,0	0,980	0,197	0,000	-0,197	0,980	-0,418	-9,693	91,401

Table 4. Measures of generalized coordinates throughout the workspace with inserted error.

Pos.	q_{11} [°]	q_{12} [°]	q_{13} [°]	q_{21} [°]	q_{22} [°]	q_{23} [°]	q_{31} [°]	q_{32} [°]	q_{33} [°]
1	278,785	-8,32	-58,88	26,73	-8,98	-42,24	143,17	0,35	-84,19
2	282,703	-24,29	-35,08	25,28	-31,43	-1,00	140,15	-11,96	-75,41
3	278,78	-45,58	1,00	26,75	-38,33	-1,00	143,15	-26,78	-48,14
4	269	-5,61	-80,48	38,88	-5,45	-53,14	141,12	-5,45	-53,14
5	269	-18,47	-71,20	41,72	-26,88	-15,17	138,28	-26,88	-15,17
6	269	-34,61	-38,74	38,89	-39,61	-1,00	141,11	-39,61	-1,00
7	259,231	-9,62	-57,14	36,88	0,93	-84,73	153,23	-8,32	-43,05
8	255,32	-26,16	-31,82	39,90	-11,36	-76,14	154,68	-31,15	-1,00
9	259,238	-45,98	1,00	36,90	-26,03	-49,30	153,21	-38,08	-1,00
10	269	-20,26	-23,67	21,82	0,35	-77,24	158,18	0,35	-77,24
11	269	-35,26	1,00	17,59	-12,14	-64,97	162,41	-12,14	-64,97
12	269	-42,06	1,00	21,85	-28,07	-38,73	158,15	-28,07	-38,73

From Equation (14) and the data of Tabs. 1 to 4 is possible estimate the geometric errors e_{pl} and the sensitivity index μ_{pl} that the structure shows when get a read of position in the workspace. The geometric errors and the index of sensitivity due to the passive revolute joints are shown in Tab. 5.

Table 5. Result geometric error and sensitivity analysis to position.

Pos.	e_{p1} [mm]	μ_{p1}	e_{p2} [mm]	μ_{p2}	e_{p3} [mm]	μ_{p3}	e_{p4} [mm]	μ_{p4}	e_{p5} [mm]	μ_{p5}	e_{p6} [mm]	μ_{p6}	e_{p7} [mm]	μ_{p7}	e_{p8} [mm]	μ_{p8}	e_{p9} [mm]	μ_{p9}
1	0,363	20,8	0,363	24,7	0,363	12,2	0,363	23,6	0,363	26,6	0,363	12,2	0,363	17,5	0,363	21,4	0,363	12,2
2	0,368	21,1	0,368	27,1	0,368	12,2	0,368	24,9	0,368	29,5	0,368	12,2	0,368	16,3	0,368	22,8	0,368	12,2
3	0,363	20,8	0,363	29,2	0,363	12,2	0,363	23,6	0,363	30,5	0,363	12,2	0,363	17,5	0,363	26,1	0,363	12,2
4	0,296	17,0	0,296	21,7	0,296	12,2	0,296	22,5	0,296	25,6	0,296	12,2	0,296	22,5	0,296	25,6	0,296	12,2
5	0,271	15,5	0,271	23,1	0,271	12,2	0,271	23,4	0,271	28,2	0,271	12,2	0,271	23,4	0,271	28,2	0,271	12,2
6	0,297	17,0	0,297	26,8	0,297	12,2	0,297	22,5	0,297	29,6	0,297	12,2	0,297	22,5	0,297	29,6	0,297	12,2
7	0,364	20,8	0,364	24,9	0,364	12,2	0,364	17,5	0,364	21,3	0,364	12,2	0,364	23,6	0,364	26,6	0,364	12,2
8	0,369	21,1	0,369	27,3	0,369	12,2	0,369	16,4	0,369	22,7	0,369	12,2	0,369	24,9	0,369	29,5	0,369	12,2
9	0,364	20,9	0,364	29,5	0,364	12,2	0,364	17,5	0,364	26,0	0,364	12,2	0,364	23,6	0,364	30,4	0,364	12,2
10	0,420	24,1	0,420	27,8	0,420	12,2	0,420	19,0	0,420	22,5	0,420	12,2	0,420	19,0	0,420	22,5	0,420	12,2
11	0,446	25,6	0,446	30,9	0,446	12,2	0,446	18,5	0,446	24,2	0,446	12,2	0,446	18,5	0,446	24,2	0,446	12,2
12	0,421	24,1	0,421	32,0	0,421	12,2	0,421	19,0	0,421	26,9	0,421	12,2	0,421	19,0	0,421	26,9	0,421	12,2

From Equation (15), the absolute error for the positions established in the Tabs. 1 to 4, are presented in Tab. 6.

Table 6. Absolute error in measuring the position, in [mm].

Pos.	1	2	3	4	5	6	7	8	9	10	11	12
e_p	0,7245	0,8181	0,9904	0,7844	0,9559	1,0772	0,8721	1,0444	1,1358	0,8535	0,9555	1,0214

Applying Equation (16) are estimate the sensitivity index μ_{ol} and geometric error e_{ol} in the measurements of orientation to the configurations established in Tabs. 1 to 4, Tab. 7.

Table 7. Result geometric error and sensitivity analysis to orientation.

Pos.	e_{o1}	μ_{o1}	e_{o2}	μ_{o2}	e_{o3}	μ_{o3}	e_{o4}	μ_{o4}	e_{o5}	μ_{o5}	e_{o6}	μ_{o6}	e_{o7}	μ_{o7}	e_{o8}	μ_{o8}	e_{o9}	μ_{o9}
1	0,029	1,7	0,029	2,3	0,029	0,5	0,029	1,6	0,029	2,8	0,029	1,0	0,029	1,1	0,029	2,2	0,029	0,7
2	0,029	1,7	0,029	2,3	0,029	0,6	0,029	1,7	0,029	3,0	0,029	1,3	0,029	1,0	0,029	2,1	0,029	0,7
3	0,029	1,7	0,029	2,2	0,029	1,0	0,029	1,6	0,029	3,0	0,029	1,3	0,029	1,1	0,029	2,4	0,029	0,8
4	0,024	1,4	0,024	1,8	0,024	0,0	0,024	1,4	0,024	2,7	0,024	1,0	0,024	1,4	0,024	2,7	0,024	1,0
5	0,022	1,3	0,022	1,6	0,022	0,1	0,022	1,4	0,022	2,9	0,022	1,2	0,022	1,4	0,022	2,9	0,022	1,2
6	0,024	1,4	0,024	1,7	0,024	0,2	0,024	1,4	0,024	2,9	0,024	1,2	0,024	1,4	0,024	2,9	0,024	1,2
7	0,030	1,7	0,030	2,2	0,030	0,4	0,030	1,1	0,030	2,2	0,030	0,7	0,030	1,6	0,030	2,8	0,030	1,0
8	0,030	1,7	0,030	2,2	0,030	0,6	0,030	1,0	0,030	2,2	0,030	0,7	0,030	1,7	0,030	3,0	0,030	1,3
9	0,030	1,7	0,030	2,1	0,030	0,9	0,030	1,1	0,030	2,4	0,030	0,8	0,030	1,6	0,030	3,0	0,030	1,3
10	0,035	2,0	0,035	2,5	0,035	0,9	0,035	1,3	0,035	2,3	0,035	0,7	0,035	1,3	0,035	2,3	0,035	0,7
11	0,037	2,1	0,037	2,6	0,037	1,2	0,037	1,3	0,037	2,3	0,037	0,6	0,037	1,3	0,037	2,3	0,037	0,6
12	0,035	2,0	0,035	2,4	0,035	1,1	0,035	1,3	0,035	2,4	0,035	0,8	0,035	1,3	0,035	2,4	0,035	0,8

Applying Eq. (17), the absolute error to the orientation established in Tabs. 1 to 4, are presented in Table 8.

Table 8. Absolute error in the measurement of orientation

Pos.	1	2	3	4	5	6	7	8	9	10	11	12
e_o	0,0782	0,0763	0,0654	0,0748	0,0701	0,0621	0,0746	0,068	0,0589	0,0755	0,0722	0,0671

From the analysis of the sensitivity index in both the measurements of position and orientation, Tabs 5 and 7, it is clear that the second joint in all legs, the joint *i*2, are those that most influence the quality measures and the third joint in all legs, the joint *i*3, are the least influences.

Based the error analysis the proposed structure 3-RRRS can be used to measure the displacements of trajectories to order of centimeters with maximum error of 1,1358mm, Tab. 6.

The absolute errors in orientation measurements should be analyzed carefully, since they indicate errors in the vector orientation of the coordinate axes of the end-effector of the 3-RRRS structure, so, small errors imply significant angular displacement. After checking through MatLab software of the rotation axis, it was found that the error in the orientation of the moving platform to the settings established by Tabs. 1 to 4, reached 4º.

3. EXPERIMENTAL TEST OF 3-RRRS STRUCTURE

To perform the test of measurement 3-RRRS structure was used a measure machine by coordinates model BR-M443M Mitutoyo with resolution of 0,5µm.

The BR-M443M is a PPPRR serial structure, i.e., from its base, its segments are connected one by one by prismatic joints, one for each Cartesian axis, giving three degrees of freedom, related to translation in any direction. The terminal element has two rotate joints, one around the ***Z*** axis, with a scale of 15º, can rotate 360 °, and the other around the axis ***X*** or ***Y***, depending on the configuration of the joint prior, with scale of 15 º, can rotate through 90 °. After making a move should lock, manually, all the joints and the displacement is shown by a computer.

To perform the experimental tests the end-effector of the 3-RRRS structure is coupled to end-effector of the BR-M443M, thus, when performing a shift, translation and / or rotation, in the end-effector of the 3-RRRS structure, this might be measured through BR-M443M, being necessary only transfer the measures to the referential of 3-RRRS structure. A picture of the system is shown in Fig. 6 (a) and the detail of the coupling of end-effector of 3-RRRS structure to the end-effector of the BR-M443M is shown in Fig. 6 (b).

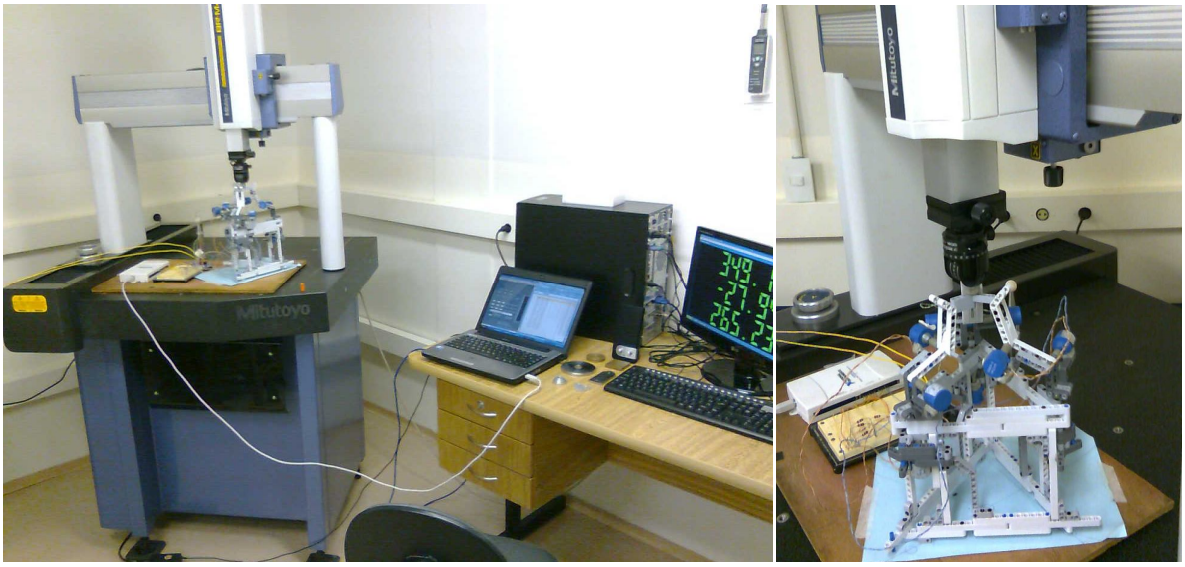

(a) (b)

Figure 6. a) Experimental System; b) Detail of the coupling of 3-RRRS structure to BR-M433 structure.

To check the validity of measurements of 3-RRRS structure and confirmation of the geometrical error analysis, experimental tests were conducted throughout the workspace of 3-RRRS structure.

The measures taken can be seen in Tab. 9, referent to translation, and in Tab. 10, referent to rotation.

It was not possible to perform rotation around the Y axis due to mechanical constraints of the 3-RRRS structure to rotation minima possible by BR-M443M.

According to Tab. 9, of the measurements made, 96,7% in the ***X*** direction, 90% in directions ***Y*** and ***Z***, are within the range obtained from the analysis of geometric errors for the position and, according to Tab. 10, all angle measurements are within expectations.

The ***Y*** direction has measures where there were major deviations and any deviations occurred with the rotation around the ***X*** axis, which may indicate the occurrence of some mechanical interference in the 3-RRRS structure during measurement.

Table 9. Measures for translational.

Pos.	BR-M433 [mm]			3-RRRS structure [mm]			Error [mm]		
	X	***Y***	***Z***	***X***	***Y***	***Z***	***X***	***Y***	***Z***
1	-5,693	-0,016	68,667	-5,010	-0,093	68,594	0,683	-0,077	-0,073
2	0,003	-0,015	66,253	-0,178	0,083	65,992	-0,182	0,097	-0,261
3	0,000	-0,015	68,665	0,028	-0,241	68,731	0,028	-0,225	0,065
4	0,003	1,964	68,665	-0,096	1,681	68,447	-0,098	-0,283	-0,218
5	0,003	-0,733	68,665	-0,035	-0,708	68,414	-0,038	0,025	-0,251
6	-2,386	-2,023	58,584	-2,002	-1,987	58,700	0,384	0,036	0,116
7	0,005	-0,199	68,670	-0,692	0,077	68,349	-0,697	0,276	-0,321
8	-4,266	-0,277	68,668	-4,410	-0,133	68,510	-0,144	0,143	-0,158
9	-3,643	3,420	68,672	-3,533	3,842	68,548	0,109	0,421	-0,123
10	-3,034	-0,420	74,072	-3,737	-0,573	74,436	-0,703	-0,153	0,364
11	-4,739	-0,420	74,072	-4,994	-0,092	74,250	-0,254	0,329	0,178
12	-0,2644	-0,0067	73,7945	-0,6352	0,3853	74,5134	-0,370786	0,392	0,7189
13	2,5991	-0,0062	72,1920	2,4345	0,4271	72,5341	-0,1646	0,4333	0,3421
14	2,5981	-0,0057	53,4085	2,5849	0,1282	54,4956	-0,0132	0,1339	1,0871
15	6,7041	-0,0067	77,2305	5,6893	-0,2934	78,1747	-1,0148	-0,2867	0,9442
16	6,708	-0,006	72,660	5,995	0,075	72,879	-0,713	0,082	0,219
17	6,708	-0,006	63,790	7,075	-0,328	64,032	0,367	-0,323	0,243
18	6,707	-0,006	55,664	7,105	-0,444	56,677	0,398	-0,438	1,013
19	4,860	-6,753	53,094	5,269	-5,949	53,484	0,409	0,804	0,390
20	-2,062	-6,754	64,744	-2,089	-6,664	64,799	-0,027	0,090	0,055
21	-2,062	-3,193	54,567	-1,946	-3,147	55,139	0,117	0,046	0,573
22	3,543	-3,193	57,857	4,574	-3,150	58,194	1,031	0,043	0,338
23	-2,3246	2,3190	68,7215	-1,1882	1,4842	67,2178	1,1364	-0,8348	-1,5037
24	-2,3251	-4,2765	58,1985	-1,5094	-6,7906	57,7120	0,8157	-2,5141	-0,4865
25	5,5569	1,9370	62,3505	5,8814	1,0643	61,6527	0,3245	-0,8727	-0,6978
26	-5,3661	1,9370	62,3500	-5,0723	1,0843	61,2057	0,2938	-0,8527	-1,1443
27	0,8354	1,9370	62,3560	1,3109	1,3710	61,1282	0,4755	-0,5660	-1,2278
28	0,8354	-5,0420	55,4615	0,9730	-7,6113	55,3411	0,1376	-2,5693	-0,1204
29	0,8354	0,2395	55,4595	1,5380	2,6215	54,9356	0,7026	2,3820	-0,5239
30	-5,693	-0,016	68,667	-5,010	-0,093	68,594	0,683	-0,077	-0,073

Table 10. Measurements of rotation.

Pos.	BR-M433 [°]			3-RRRS structure [°]			Error [°]		
	X	***Y***	***Z***	***X***	***Y***	***Z***	***X***	***Y***	***Z***
1	0	0	0	-0,86	0,77	0,62	-0,86	0,77	0,62
2	0	0	0	0,26	1,18	0,89	0,26	1,18	0,89
3	0	0	0	0,08	-0,20	1,19	0,08	-0,20	1,19
4	0	0	0	-0,74	0,37	0,93	-0,74	0,37	0,93
5	0	0	0	0,36	0,60	0,21	0,36	0,60	0,21
6	0	0	0	1,07	-0,11	0,75	1,07	-0,11	0,75
7	0	0	0	0,80	0,66	0,82	0,80	0,66	0,82
8	0	0	0	0,26	-0,72	0,28	0,26	-0,72	0,28
9	0	0	0	-0,81	-0,88	0,69	-0,81	-0,88	0,69
10	0	0	0	0,38	0,98	0,97	0,38	0,98	0,97
11	0	0	0	0,63	-0,10	0,80	0,63	-0,10	0,80
12	0	0	-15	0,50	-1,40	-14,42	0,50	-1,40	0,58
13	0	0	-15	-0,60	-0,96	-15,58	-0,60	-0,96	-0,58
14	0	0	-15	-0,02	-0,50	-13,96	-0,02	-0,50	1,04
15	0	0	-15	-0,29	1,28	-15,44	-0,29	1,28	-0,44
16	0	0	-15	0,40	1,71	-14,83	0,40	1,71	0,17
17	0	0	-15	0,42	0,85	-17,58	0,42	0,85	-2,58
18	0	0	-15	0,80	0,62	-16,25	0,80	0,62	-1,25
19	0	0	-15	1,92	-0,48	-14,56	1,92	-0,48	0,44
20	0	0	-15	0,56	-3,87	-13,49	0,56	-3,87	1,51
22	0	0	-15	0,69	-3,52	-13,02	0,69	-3,52	1,98
23	0	0	-15	0,64	-1,11	-16,48	0,64	-1,11	-1,48
24	-15	0	0	-13,10	-1,43	-3,05	1,90	-1,43	-3,05
25	-15	0	0	-15,30	-0,72	-2,91	-0,30	-0,72	-2,91
26	-15	0	0	-12,87	2,29	-2,68	2,13	2,29	-2,68
27	-15	0	0	-12,61	-3,29	-2,74	2,39	-3,29	-2,74
28	-15	0	0	-12,17	0,08	-1,56	2,83	0,08	-1,56
29	-15	0	0	-14,79	0,64	-1,35	0,21	0,64	-1,35
30	-15	0	0	-13,77	0,87	-1,01	1,23	0,87	-1,01

4. CONCLUSION

In this paper was developed an electro-mechanical system using as the base the parallel structure 3-RRRS for measuring robot path.

First the structure proposed to measuring robot path was presented. After the geometric model, Jacobian matrix and the analysis of geometric errors were performed.

The experimental tests were realized using a measure machine by coordinates model BR-M443M Mitutoyo with resolution of 0,5µm. The results show, that according to the analysis of errors and the components used, the proposed structure can be used to verify the position and orientation of a trajectory defined by a given robotic structure.

For future works will be carried out tests on an industrial robot with 6 degrees of freedom and the construction of an improved structure with the use of more accurate sensors.

5. ACKNOWLEDGEMENTS

The authors are thankful to Dimensional Metrology Laboratory of UFU/FEMEC, CNPq, CAPES and FAPEMIG for the partial financing support of this research work.

6. REFERENCES

Alves, A. S. , 1996, “Metrologia Geométrica”, Lisboa, Fundação Calouste Gulbenkian, 269 p.

Kim, J.-A., Bae, E. W., Kim, S. H. and Kwak, Y. K., 2002, “Design methods for six-degree-of-freedom displacement measurement systems using cooperative targets”, Journal of the International Societies for Precision Engineering and Nanotechnology, Vol. 26, pp. 99-104.

Fan, K.-C. and Chen, M.-J., 2000, “A 6-degree-of-freedom measurement system for the accuracy of X-Y stages”, Journal of Elsevier Science Inc., Precision Engineering, Vol. 24, pp. 15-23.

Gonçalves, R. S., 2009, "Estudo de rigidez de cadeias cinemáticas fechadas”, Thesis, Federal University of Uberlândia, Brazil.

Oliveira Jr., A. A. and Carvalho, J. C. M., 2002, “A Modified Stewart Platform for Measuring Robot Path”, MUSME 2002, The International Symposium On Multibody System and Mechatronics, Mexico.

Tsai, L.W., 1999, “Robot Analysis: The Mechanics of Serial and Parallel Manipulators”, John Wiley & Sons, New York, pp.260-297.

Zangl, H., Bretterklieber, T., Steiner, G. and Riedmuller, K., 2007, “Feasibility Study for a Three-Axial joystick based on an Array of Lateral Hall Elements”, IEEE SENSORS 2007 Conference.

Wu, C.-M. and Chuang, Y.-T., 2004, “Roll angular displacement measurement system with microradian accuracy”, Journal of Elsevier Science Inc., Sensors and Actuators, Vol. A 116, pp. 145-149.

7. RESPONSIBILITY NOTICE

The authors are the only responsible for the printed material included in this paper.